Model of a ternary complex between activated factor VII, tissue factor and factor IX

Shu-Wen W Chen, Jean-Luc Pellequer, Jean-François Schved, Muriel Giansily-Blaizot

Model of a ternary complex between activated factor VII, tissue factor and factor IX.

Shu-wen W. Chen, Jean-Luc Pellequer[1,2] Jean-François Schved[3], Muriel Giansily-Blaizot[3]

From the [1]CEA Valrhô – Site de Marcoule. DSV/DIEP/SBTN, BP 17171 30207 Bagnols-sur-Cèze, France. [2]The Department of Molecular Biology, The Scripps Research Institute, 10550 N. Torrey Pines Road, La Jolla, CA 92037 USA. [3]Laboratoire d'hématologie, CHU Saint-Eloi, 34295 Montpellier, France.

Running title : FVIIa:TF:FIX ternary complex.

Keywords: Protein-protein interaction, haemostasis, coagulation cascade, haemophilia, extrinsic pathway, comparative modeling, homology modelling.

Send all correspondence to: Jean-Luc Pellequer, Institut de Biologie Structurale, 71 avenue des Martyrs, CS10090, 38044 Grenoble Cedex 9, France.

Tel: +33 (0)457 42 8756 Fax: +33 (0)476 50 1890 email: jlpellequer@cea.fr

and Muriel Giansily-Blaizot Laboratoire d'hématologie, CHU Saint-Eloi, 34295 Montpellier, France; email: m-giansily@chu-montpellier.fr

Summary

Upon binding to tissue factor, FVIIa triggers coagulation by activating vitamin K-dependent zymogens, factor IX (FIX) and factor X (FX). To understand recognition mechanisms in the initiation step of the coagulation cascade, we present a three-dimensional model of the ternary complex between FVIIa:TF:FIX. This model was built using a full-space search algorithm in combination with computational graphics. With the known crystallographic complex FVIIa:TF kept fixed, the FIX docking was performed first with FIX Gla-EGF1 domains, followed by the FIX protease/EGF2 domains. Because the FIXa crystal structure lacks electron density for the Gla domain, we constructed a chimeric FIX molecule that contains the Gla-EGF1 domains of FVIIa and the EGF2-protease domains of FIXa. The FVIIa:TF:FIX complex has been extensively challenged against experimental data including site-directed mutagenesis, inhibitory peptide data, haemophilia B database mutations, inhibitor antibodies and a novel exosite binding inhibitor peptide. This FVIIa:TF:FIX complex provides a powerful tool to study the regulation of FVIIa production and presents new avenues for developing therapeutic inhibitory compounds of FVIIa:TF:substrate complex.

Introduction

Activated factor VII / tissue factor (FVIIa:TF) enzyme complex is the principal initiator of the coagulation cascade. FVIIa has little proteolytic activity on its own (1). However, when complexed to the tissue factor (TF), FVIIa triggers coagulation by activating vitamin K-dependent zymogens, factor IX (FIX) and factor X (FX) to their respective active forms FIXa and FXa (2,3). The FVIIa:TF complex can also activate FVII in an autocatalytic manner (4) but it remains unclear to what extent this pathway contributes to the generation of FVIIa. Vitamin K-dependent factor VII (FVII), factor IX, factor X, and protein C are highly homologous proteins made up of four domains: a carboxyglutamic acid (Gla)-rich domain at the N terminus, then two epidermal growth factor (EGF)-like domains, and a chymotrypsin-type serine protease domain at the C terminus. Because FVII, FIX, and FX share significant structural homology, these substrates are likely to bind in a similar fashion onto FVIIa:TF and therefore binding data pertaining to a particular substrate might be applied to others (5).

FVIIa:TF initiated coagulation is involved in various pathological conditions including cardiovascular atherosclerotic disease (6-8), disseminated intravascular coagulation (9) and probably venous thrombosis (10). Thus, analysis of the ternary complex TF:FVIIa:substrate, with substrate being either FIX, FX or FVII itself, may have important implications for potential development of anticoagulant therapies. In the absence of crystallographic complex, we have performed docking experiments to identify substrate binding residues and to predict the orientation of FVIIa relative to its substrates.

Despite an explosion in available experimentally-determined protein structures, protein-protein complexes remain scarce in the Protein Data Bank (11). Alternatively, protein docking is a computational technique aiming at predicting protein-protein interactions (12,13). In a blind test,

several algorithms were used to predict the binding of the β-lactamase inhibitory protein to the TEM-1 β-lactamase (14). Each of the six participating research groups predicted the correct general mode of association, highlighting the maturity of these algorithms (14). However, to be feasible, protein docking requires common approximations. Most often proteins are kept rigid rigid (15-17) although local refinements have shown improved results (18,19). To take into account side-chain flexibility, shape-based search protocols (20-22) use a qualitative "softness" in the shape potential with a simplified van der Waals and electrostatic scoring functions (23-26).

Because of the intrinsic flexibility of vitamin K-dependent coagulation factors, we need to take into account flexibility in our docking experiment. Due to the large structural similarity found among domains of vitamin K-dependent coagulation factors (27), we built chimeric protein structures of FIX. We present a molecular docking experiment between FVIIa:TF and a chimeric FIX that contains either the Gla-EGF1 domains from FVIIa (28), or the Gla-EGF1 domains from FIXa (29) followed by the EGF2-protease domains of FIXa (Code 1PFX). The rationale for using chimeric proteins in docking is that we take advantage of known experimental conformation of domains rather than introduce a flexibility parameter in the three-dimensional conformational search space. In addition, the Gla domain of the FIXa crystal structure was not well ordered in the electron density and was therefore modeled in the structure 1PFX. Consequently, the Gla domain present in this crystal structure might be an inappropriate form of molecular docking with FVIIa:TF. Here, we focus on the flexibility between the Gla and EGF1 domains. It has been shown that EGF1 domains of FVII, FIX and FX are involved in FVIIa:TF binding (30-33). In addition, Gla domains anchor onto phospholipid membranes using solvent-exposed hydrophobic side-chains (34-36). Therefore Gla domain of FIX is expected to be in the same putative membrane plane as the Gla domain of FVIIa:TF complex. Such biochemical information is often critical in determining the correct binding mode of a protein (23). To perform our docking experiments, we used the DOT program

(37) which is a grid-based, six-dimensional search algorithm that computes interaction energies between a fixed and a moving molecule as a correlation function rapidly calculated using fast fourier transforms (25,37,38), similar to the algorithm that outperforms other programs during the β-lactamase blind test (14,20). In combination with computational graphics, DOT runs allow us to present a putative ternary complex FVIIa:TF:FIX that has been extensively challenged against known experimental data. Our chimeric protein docking approach is useful in the mist of the post-genomic era where the number of experimentally determined structures of paralogs will exponentially increase, giving us alternate conformations of multi-domain protein families.

Methods

Preparation of coordinate files

The coordinates of the FVIIa:TF complex (28) (code 1DAN) and FIXa (29) (code 1PFX) were obtained from the Protein Data Bank (11). Calcium ions in the X-ray diffraction determined structures were kept. Hydrogen atoms were built using X-PLOR software (39) and the energy was minimized according to the CHARMM22 force field parameters (40). Histidine residues were positively charged when exposed to solvent and otherwise were electrically neutral with protonated NE2 atoms. The coordinates of all atoms were generated relative to the center of atomic positions of the molecule where all non-polar hydrogen atoms were previously removed. Chymotrypsin numbering has been retained for all coagulation factors where the prefix L indicates light chain and the prefix H the heavy chain. Numbering according to zymogen proteins is systematically indicated in parentheses for FVII (41), FIX (42), and FX (43).

The system of ternary complex docking

The DOT program searches the binding site on the molecular surface of a protein by systematically rotating and translating another protein around it. Both proteins are treated as rigid bodies. In the present study, the FVIIa:TF complex was assigned as the stationary molecule and FIX Gla-EGF1 as the moving one. Due to the large size of the stationary molecule, we used a truncated FVIIa including residues from L1 to L95 and a complete set of TF coordinates for the FIX Gla-EGF1 docking. The last residue, L95, was not modified with a C-terminal carboxylated group to prevent truncation artefact. Both molecules were initially located at the center of the grid box for running DOT.

Binding energy calculations of the FVIIa-TF complex and FIX Gla-EGF-1

We evaluated the binding energy of the ternary complex as the composite sum of electrostatic and van der Waals energies. In the DOT program, electrostatic energy is expressed as a correlation function of electrostatic potential exerted by the stationary molecule and the charge density of the moving molecule. Similarly, the van der Waals energy is the correlation function of the van der Waals potential of the stationary molecule and the atomic position of the moving molecule. Energies were calculated at each grid point in the box. We used a 128x128x128 grid with 1 Å spacing, a dielectric of 3 for protein interior, a dielectric of 80 for the aqueous environment, a temperature of 300 K, an ionic exclusion radius of 1.4 Å, and a solvent radius of 1.4 Å. The salt effect was represented by a solvent ionic strength of 150 mM.

Partial charges of atoms for both stationary and moving proteins were taken from the AMBER library. The net charge of the truncated FVIIa-TF complex is zero and that of FIX Gla-EGF-1 is 4 positive electronic units. To alleviate the artefact due to singularities occurring when calculating electrostatic energies, we clamped all values of the electrostatic potential grid of the stationary molecule in the range –7 to +7 Kcal/mol/e. All electrostatic potentials at grid points were obtained by solving the Poisson-Boltzmann equation.

In a van der Waals potential grid of the stationary molecule, grid points in the “surface layer” (1.5 to 4.5 Å from a non-hydrogen atomic center) were assigned a value of 1, while those penetrating the van der Waals volume of a non-hydrogen atom (within 1.5 Å to the atomic center) were assigned a highly unfavorable value of 1000. All other grid points were assigned a value of zero. To scale the atom counts of the moving molecule lying within the surface layer to an energetic term, we chose a van der Waals well depth of –0.1 Kcal/mol for all interactions and eliminated the grid points with collisions greater than zero. DOT runs in parallel on 25 computers (Sun Ultra) in about 8.5 hours cpu time.

Results

Chimeric FIX docking

We performed two docking experiments. In the first, the Gla-EGF1 domains of FIXa were used as a moving molecule; and in the second, we modeled new Gla-EGF1 domains of FIX using the Gla-EGF1 domains of FVIIa and used this chimeric construction as a moving molecule. The main difference between these two structures is located in the angle between the Gla domain and the EGF1 domain (about a 90° difference). DOT generates a minimum-energy grid in which the lowest interaction energy among the 28800 rotations is saved at each grid point. To analyze these 2,097,152 values we calculated an iso-potential surface from the minimum-energy grid that reveals "best" clusters with the lowest binding energy. Large clusters have been often correlated with correct binding sites (25). Unfortunately, no large low-energy cluster has been found either for the first or for the second docking experiments. This is quite common when molecules contain significant flexibility. Moreover, the membrane is not included in the search and therefore part of the interaction energy between physiological FIX and FVIIa:TF is missing. We then analysed in detail the top 2000 answers. To screen potential docking solutions, we selected those having their FIX Gla domain in the same plane as the FVIIa Gla domain using computational graphics. Only solutions of the second run satisfied this knowledge-based requirement. Putative docked FIX conformation includes solutions ranked #1, #258, #474, #1241, #1845, ranked according to their binding energies. These five conformations are located within 2 Å distance on the grid. It should be noted that no solution from the first run is found close in space to the solution ranked first of the second run, even in the top 2000 answers.

FIX Gla-EGF1 docking orientation

The Gla domain from the solution ranked first of the second run is oriented 90 degrees relative to the FVIIa Gla domain of the FVIIa:TF complex. Solvent-exposed hydrophobic side-chains (grey coloured residues) of FVIIa and FIX are located on a same plane (yellow) which represents the putative membrane (Fig. 1A). The FIX Gla domain is located beneath, but slightly shifted toward the front (Fig. 1). This slight shift allows the C-terminal peptide of physiological TF to reach the membrane without steric constraints from the FIX Gla domain. Schematically, the FIX EGF1 β-sheet domain from the solution ranked first of the second run and the C-terminal fibronectin type III domain of TF share contiguous areas. In such an orientation, FIX EGF1 could make backbone hydrogen bonds with backbone atoms from TF, though no further optimization of such hydrogen bonds has been performed. The FIX Gla and EGF1 domains make several contacts with TF (Fig. 1). Our docking indicates that TF Ile152, Tyr157, Lys159, Ser161, Ser162, Ser163, Gly164, Lys165, Lys166, Thr167, Lys169, Asp180, Asn184, Pro194, and Ser195 are in direct contact with several residues from FIX: LeuL14, CguL15, MetL19, CguL20, PheL41, TyrL45, GlyL48, AspL49, GluL52, AsnL54, GlyL59, SerL61, LysL63, AspL64, ProL74, PheL75. The total buried molecular surface area between FVIIa:TF and FIX Gla-EGF1 domains is 1033 $Å^2$ including 844 $Å^2$ between TF and FIX Gla-EGF1 domains. FIX Gla domain makes direct contact with the Gla domain of FVIIa. In particular, residue ArgL36 from FVIIa participates in a triple hydrogen-bond network (Fig. 1) with backbone carbonyl oxygen from residues Ser163 (TF), MetL19 and CguL20 (FIX Gla domain). Hydrogen bonds or salt bridges are made between FIX LysL63 and TF Tyr157, FIX AspL64 and TF Lys166, FIX AspL49 and TF Lys166, and FIX AsnL54 and TF Lys169. Residues making salt-bridges, hydrogen bonds or van der Waals contacts are quite conserved in all substrates FVII, FIX, FX (Fig. 2). In grey background are represented residues conserved in all four vitamin K-dependent coagulation factors. Interestingly, FIX AsnL54 is found near a region that differs significantly between coagulation factors VII, IX, X, and APC. In APC, which does not bind to FVIIa:TF, a long insertion (eight residues) is found between residues FIX ProL55 and CysL56.

In addition, APC significantly differs from FVIIa:TF substrates at several positions found in direct contact with TF highlighted in white in Fig. 2. Our docking suggests that the long insertion in APC compared with other vitamin K-dependent substrates of FVIIa:TF is located at the interface between EGF1 and TF, therefore preventing APC from binding to FVIIa:TF.

Docking of a complete FIX molecule

To complete the FIX docking onto FVIIa:TF, the position of FIX protease domain remains to be determined. Two knowledge-based constraints are known. Firstly, the N-terminal activation peptide (AP) of FIX protease domain binds onto the active site of FVIIa in which FIX Arg(180) will be cleaved, thus producing FIXa. Secondly, the FIX EGF2 domain must be covalently bound to the EGF1 domain that has been previously docked. We observed that little flexibility is found between EGF2 and protease domains of vitamin K-dependent coagulation factors (44). Thus, we treated FIX EGF2 domain as an integral part of the protease domain during the next docking experiment.

To model FIX AP into the FVIIa active site, we superimposed the FVIIa crystal structure bound to the bovine pancreatic trypsin inhibitor (45) (code 1FAK) onto the FVIIa crystal structure bound to TF used in our docking (code 1DAN). Then, residues from P4 to P4' of the trypsin inhibitor were transferred to their respective positions in FVIIa:TF structure and assigned to residues P4 to P4' of FIX AP. A complete model of FIX AP has been presented elsewhere, however, in an unbound conformation (46). Then, we performed a full space search docking experiment with FIX serine protease (with EGF2 but without the activation peptide) as a moving molecule and the FVIIa (from the FVIIa:TF complex) as a fixed molecule. Since DOT uses a complete treatment of electrostatic interactions, Ca^{2+} ions were included during our docking. Since no large cluster of FIX were found around FVIIa, we analysed the top 2000 answers, to search for FIX serine protease domain orientation that is compatible with the two aforementioned constraints (AP and EGF1 connection). We identified the solution ranked #17 and used computational graphics to further optimize this

orientation. In particular we modeled the connection between EGF1 and EGF2 in an extended conformation (Fig. 3A). Several cycles of refinement were performed to energy-minimize our docking and to optimize amino-acid geometry. No further refinement concerning specific side-chain side-chain interactions were pursued.

In the final model, the total buried surface area between FIX heavy chain and FVIIa:TF is 1071 $Å^2$ whereas the total buried area between FIX light chain and FVIIa:TF is 1033 $Å^2$. Considering the pseudo-plane made by the FVIIa and FIX Gla domains, FIX catalytic triad is located about 100 Å above the membrane (compared to 95 Å for FVIIa active site). Fig. 3 displays the complete ternary complex. FIX active site is located on the opposite side of FIX AP and regions involved in FX binding are coloured yellow in Fig. 3B. Fig. 3C presents a schematic drawing of the interactions found in the FVIIa:TF:FIX complex.

Discussion

In the absence of crystallographic data, full-space search algorithms are promising methods to predict protein-protein interactions. Our goal was to dock a complete inactivated coagulation factor FIX (FIX) onto the crystallographic complex of activated factor VII (FVIIa):tissue factor (TF); thus providing a complete picture of the first event of the extrinsic pathway in the blood coagulation cascade. To dock the flexible multi-domain FIX protein (Gla, EGF1, EGF2, protease domain), we proceeded in two steps. First, we determined a proper docking orientation for FIX Gla-EGF1 domains onto FVIIa:TF. Then, we docked the FIX EGF2-protease domains using structural constraints such as the location of FIX EGF1-Gla domain and FIX activation peptide. The rationale for starting the complete docking of FIX by the Gla-EGF1 domains is that a strong constraint exists for FIX Gla domain. Indeed, Gla domains are known to bind to membranes using solvent-exposed hydrophobic side-chains (34-36) and therefore FIX Gla domain should be located in approximately the same plane as the Gla domain of FVIIa.

Vitamin K-dependent coagulation factors are very flexible proteins (27,44). To overcome this flexibility using a full space search rigid docking algorithm, we used two conformations of FIX Gla-EGF1 domains. The first FIX Gla-EGF1 domain is found in the FIXa crystal structure (29) whereas the second Gla-EGF1 domain was built using the Gla-EGF1 domains of FVIIa found in the FVIIa:TF crystal structure (28); creating a so-called chimeric FIX. One docking experiment was performed with each FIX construction yielding only to a satisfactory docking with the second construction. Although it may be fortuitous that, in the second construction, the conformation of FIX Gla-EGF1 domains was the solution ranked first using the DOT interaction energy function, we will now present compelling experimental evidence that support our docking conformation of the whole FIX onto FVIIa:TF. These experimental data were obtained from synthetic peptide inhibition, site-directed mutagenesis and haemophilia mutation databases, neutralizing antibody

binding sites (epitopes), and novel peptide-based anticoagulant inhibitors. It must be emphasized that none of these experimental data were used to build the initial complex since the FIX Gla-EGF1 orientation was determined solely by the automated DOT program. Because vitamin K-dependent coagulation factors VII, IX, X are structurally similar and since it has been shown that FIX and FX interact with the same TF region in the FVIIa:TF complex (47), we decided to concurrently analyze experimental data from each substrate in the following discussion.

Synthetic peptide inhibition

Non competitive inhibition of FX activation revealed that FVII H142-H163(285-305) was the most inhibitory peptide with a Ki value of 2.4 µM (48) suggesting that peptide H142-H163(285-305) is located at the interface between FVIIa and FIX. In our FVIIa:TF:FIX complex, the buried molecular surface between FVIIa H142-H163(285-305) and FIX is about 195$Å^2$ representing about 20% of the total buried molecular surface of FIX protease domain. Such contact surface area is in agreement with inhibition data suggesting that FVII H142-H163(285-305) is located at the interface between FVIIa:TF and its molecular substrate (red CPK in Fig. 3A).

In addition, several studies have identified FIXa peptides involved in FX activation on the intrinsic tenase complex (49-52). These peptides are located around the catalytic cleft of FIXa. On our model, these peptides (and FIX catalytic cleft) are located on the back side of FIX when interacting with FVIIa:TF complex (yellow CPK in Fig. 3B).

Site-directed mutagenesis and database mutations

Mutations characterized on FVIIa, TF, or FIX were analysed to challenge our FVIIa:TF:FIX docking. Site-directed mutations performed in the FVIIa Gla domains identified a critical residue ArgL36 (32). It was shown that FVIIa ArgL36 is involved in the recognition process with macromolecular substrate FX Gla-domain and TF. A previous molecular docking of FX Gla

domain onto FVIIa:TF did not provide a satisfying structural explanation for the role of ArgL36 (32). In our docking, ArgL36 is involved in a triple interaction with TF and FIX Gla domains (Fig. 1B) in agreement with the important role of ArgL36.

It has been shown that FVIIa GluH154(296) influences the linkage of the macromolecular substrate binding site to the catalytic center through an unknown mechanism (53). In our docking complex, FVIIa GluH154(296) makes a salt bridge with FIX ArgH188A(358). Among FVIIa:TF substrates, a positively charged residue is found at position H188A(358) in both FIX and FVII. In FX, LysH186(370) or LysH156(338) could play a similar role since in our model H186 of FIX is 9 Å away from FVIIa GluH154(296) and H156 is 12 Å away from FVIIa GluH154(296), compared to 9 Å between FIX ArgH188A(358) and FVIIa GluH154(296) (Cα distances). The observed allosteric effect of FVIIa GluH154Ala(296) mutation could proceed from a molecular switch turned on when FVIIa:TF binds to its molecular substrate.

FVIIa ArgH147(290) has been shown to be required for efficient activation of the macromolecular substrate FX and other serine protease substrates FVII and FIX (54). In our ternary complex FVIIa ArgH147(290) makes a hydrogen bond with FIX light chain SerL138 and with FIX GlnH26(191) from the protease domain. Among FVII, FIX, FX, position H26 is very conserved with either a Gln or a Glu, both able to make a hydrogen bond or a salt bridge with FVIIa ArgH147(290). No other polar residues are located surrounding FIX GlnH26(191) making this position the principal interaction target for ArgH147(290). Unfortunately, the only natural missense mutation reported in the haemophilia B database, Gln191Lys, is cross-reacting material negative (CRM-) and certainly proceeds from another mechanism.

On the other hand, analysis of two CRM+ FIX mutations Gly48Arg and Gly48Val have revealed that these FIX mutants were barely activated by the FVIIa:TF complex (55). Our FVIIa:TF:FIX complex indicates that FIX GlyL48 is located on the interface with TF and therefore the replacement of Gly by a bulkier amino acid (Arg or Val) may prevent binding of FIX onto

FVIIa:TF (Fig. 1). Another mutation in the FIX haemophilia database, Arg94Ser in the second EGF domain, is characterized by a FIX with a 20-fold reduced FVIIa:TF activation due to the presence of an additional O-linked carbohydrate (56). In our model, ArgL94 is located about 15-20 Å from FVIIa:TF. Therefore, a bulky O-linked carbohydrate could prevent a productive association between FIX and FVIIa:TF.

Site-directed mutations performed on TF provide additional information on FIX binding. A reduced activation of FIX and FX has been found for TF mutants Lys165Ala and Lys166Ala (57,58). In addition, mutation analysis on TF Ser162, Ser163 and Tyr157 revealed that these residues are involved in the binding interface with FIX or FX (59). Our docking confirms that several residues in FIX Gla-EGF1 domains are involved in binding of TF (Fig. 1). An alanine scan of TF solvent-exposed residues has delineated those of TF (Tyr157, Lys159, Ser163, Gly164, Lys165, Lys166, and Tyr185) that bind to FIX or FX (47). In our docking, most of these residues make specific contacts with FIX residues (Fig. 1) and each residue is located in the interface between FVIIa:TF and FIX.

In summary, the orientation of FIX relative to FVIIa:TF is supported by mutation data found in the FIX Gla-EGF1 and protease domains as well as mutations found in FVIIa and tissue factor. In addition, our ternary complex provides new testable hypotheses for specific residue-residue interactions.

Antibody binding sites

Monoclonal antibodies are exquisite tools to characterize protein-protein interaction. Six anti-TF monoclonal antibodies have been described (60,61). Among them 7G11, 6B4, and HTF1 do not display significant anticoagulant potencies (62). Epitope mapping of antibodies D3H44 and 5G6, that showed potent anticoagulant properties, revealed that residues TF Lys165, Lys166, Asn199, Arg200, and Lys201 are critical epitope residues (61). Epitope of another potent anti-human-TF

monoclonal antibody, 5G9 (60) for which a crystal structure has been determined in complex with TF, has been mapped to residues Tyr156, Lys169, Arg200 and Lys201 (63) (code 1AHW). Because antibody 5G9 is a competitive inhibitor for macromolecular substrate FX activation and because 5G9 epitope overlaps with D3H44 and 5G6 epitopes, D3H44 and 5G6 are likely competitive inhibitors for FVIIa:TF. The location of the 5G9 epitope was displayed onto our ternary complex model (Fig. 4A). Taking the volume occupied by an antibody into account, our FIX docking is in agreement with the competitive inhibition mechanism through steric hindrance, explaining their anticoagulant properties.

Three monoclonal antibodies have been raised against the serine protease domain of FVIIa. Antibodies 12C7 and 12D10 share a common binding site and bind to FVIIa with a sub-nanomolar affinity in the presence or absence of TF, whereas antibody F3-3.2A binds with a lower affinity (64). Antibody F3-3.2A inhibits proteolytic activity of FVIIa:TF by competition with FX for binding to FVIIa:TF. The epitope of antibody F3-3.2A is mapped on our ternary complex and overlaps significantly with FIX binding site onto FVIIa:TF (red in Fig 4B). In our model, epitopes of antibodies 12C7 and 12D10 do not overlap with FIX binding site onto FVIIa:TF (yellow in Fig. 4) in agreement with the inhibition mode observed for these two antibodies (64).

Exosite peptides

A novel class of peptide exosite inhibitors of FVIIa has been recently developed (65). Using peptide libraries, peptide E-76 was selected as a potent anticoagulant inhibitor. E-76 binds to FVIIa and non-competitively inhibits activation of FX and amidolytic activity. A crystal structure of E-76:FVIIa complex was determined (65) revealing a large conformational change in FVIIa loop H142-H154. The inhibitor E-76 does not prevent substrates to bind (FX), but strongly affect the activation process. Our ternary complex enables us to suggest a molecular inhibition mechanism of E-76 that corresponds with their observation. Fig. 5 shows our FVIIa:TF:FIX complex in which the

large conformational change observed in E-76:FVIIa complex is superimposed. It appears that the conformation of FVIIa loop H142-H154 in the E-76:FVIIa complex overlaps with the activation peptide of FIX. Therefore, E-76 inhibition mode is to prevent processing of the scissile bond of substrate FIX by blocking the access of the activation peptide tail from the FVIIa active site.

Therapeutic perspective

A self amplifying pathway regulated by feed forward and backward loops offers new possibilities for developing antagonisms other than direct inhibition of the resulting thrombin protease. Preventing thrombosis and thrombotic complications by inhibiting FVIIa:FT complex activity have already been proposed either using RNA aptamers directed against FVIIa (66), monoclonal antibodies against TF (67), FVII/FVIIa (68) and FIX (69) or active site-inhibited FVIIa (70-72). Moreover, anticoagulants that directly target thrombin are often associated with severe haemorrhagic complications, whereas FVIIa:TF complex antagonists showed reduced bleeding in animal models (73,74). This might be explained by the fact that inhibition of the FVIIa:TF complex does not compromise thrombin activity but limits the generation of upstream procoagulant factors respecting the regulating loop. Computational prediction of the TF:FVIIa:FIX complex will offer new targets for the development of inhibitors and new anti-thrombotic agents.

Acknowledgements

This research was supported by a NIH fellowship HL07695 (to JLP). JLP thanks Victoria Roberts for fruitful discussions concerning the DOT program.

References

1. Lawson, JH, Butenas, S, Mann, KG. The evaluation of complex-dependent alterations in human factor VIIa. J Biol Chem 1992; 267: 4834-43.
2. Osterud, B, Rapaport, SI. Activation of factor IX by the reaction product of tissue factor and factor VII: additional pathway for initiating blood coagulation. Proc Natl Acad Sci U S A 1977; 74: 5260-4.
3. Cooper, DN, Millar, DS, Wacey, A, Banner, DW, Tuddenham, EG. Inherited factor VII deficiency: molecular genetics and pathophysiology. Thromb Haemost 1997; 78: 151-60.
4. Yamamoto, M, Nakagaki, T, Kisiel, W. Tissue factor-dependent autoactivation of human blood coagulation factor VII. J Biol Chem 1992; 267: 19089-94.
5. Ellison, EH, Castellino, FJ. Adsorption of vitamin K-dependent blood coagulation proteins to spread phospholipid monolayers as determined from combined measurements of the surface pressure and surface protein concentration. Biochemistry 1998; 37: 7997-8003.
6. Marmur, JD, Thiruvikraman, SV, Fyfe, BS, Guha, A, Sharma, SK, Ambrose, JA, Fallon, JT, Nemerson, Y, Taubman, MB. Identification of active tissue factor in human coronary atheroma. Circulation 1996; 94: 1226-32.
7. Hasenstab, D, Lea, H, Hart, CE, Lok, S, Clowes, AW. Tissue factor overexpression in rat arterial neointima models thrombosis and progression of advanced atherosclerosis. Circulation 2000; 101: 2651-7.
8. Westmuckett, AD, Lupu, C, Goulding, DA, Das, S, Kakkar, VV, Lupu, F. In situ analysis of tissue factor-dependent thrombin generation in human atherosclerotic vessels. Thromb Haemost 2000; 84: 904-11.

9. Asakura, H, Kamikubo, Y, Goto, A, Shiratori, Y, Yamazaki, M, Jokaji, H, Saito, M, Uotani, C, Kumabashiri, I, Morishita, E, et al. Role of tissue factor in disseminated intravascular coagulation. Thromb Res 1995; 80: 217-24.

10. Semeraro, N, Colucci, M. Tissue factor in health and disease. Thromb Haemost 1997; 78: 759-64.

11. Berman, HM, Westbrook, J, Feng, Z, Gilliland, G, Bhat, TN, Weissig, H, Shindyalov, IN, Bourne, PE. The Protein Data Bank. Nucleic Acids Res. 2000; 28: 235-42.

12. Janin, J. Protein-protein recognition. Prog Biophys Mol Biol 1995; 64: 145-66.

13. Sternberg, MJ, Gabb, HA, Jackson, RM. Predictive docking of protein-protein and protein-DNA complexes. Curr Opin Struct Biol 1998; 8: 250-6.

14. Strynadka, NC, Eisenstein, M, Katchalski-Katzir, E, Shoichet, BK, Kuntz, ID, Abagyan, R, Totrov, M, Janin, J, Cherfils, J, Zimmerman, F, Olson, A, Duncan, B, Rao, M, Jackson, R, Sternberg, M, James, MN. Molecular docking programs successfully predict the binding of a beta- lactamase inhibitory protein to TEM-1 beta-lactamase. Nat Struct Biol 1996; 3: 233-9.

15. Goodsell, DS, Olson, AJ. Automated docking of substrates to proteins by simulated annealing. Proteins 1990; 8: 195-202.

16. Jiang, F, Kim, SH. "Soft docking": matching of molecular surface cubes. J Mol Biol 1991; 219: 79-102.

17. Cherfils, J, Duquerroy, S, Janin, J. Protein-protein recognition analyzed by docking simulation. Proteins 1991; 11: 271-80.

18. Totrov, M, Abagyan, R. Detailed ab initio prediction of lysozyme-antibody complex with 1.6 A accuracy. Nat Struct Biol 1994; 1: 259-63.

19. Jackson, RM, Gabb, HA, Sternberg, MJ. Rapid refinement of protein interfaces incorporating solvation: application to the docking problem. J Mol Biol 1998; 276: 265-85.

20. Katchalski-Katzir, E, Shariv, I, Eisenstein, M, Friesem, AA, Aflalo, C, Vakser, IA. Molecular surface recognition: determination of geometric fit between proteins and their ligands by correlation techniques. Proc Natl Acad Sci U S A 1992; 89: 2195-9.

21. Walls, PH, Sternberg, MJ. New algorithm to model protein-protein recognition based on surface complementarity. Applications to antibody-antigen docking. J Mol Biol 1992; 228: 277-97.

22. Helmer-Citterich, M, Tramontano, A. PUZZLE: a new method for automated protein docking based on surface shape complementarity. J Mol Biol 1994; 235: 1021-31.

23. Gabb, HA, Jackson, RM, Sternberg, MJ. Modelling protein docking using shape complementarity, electrostatics and biochemical information. J Mol Biol 1997; 272: 106-20.

24. Vakser, IA, Matar, OG, Lam, CF. A systematic study of low-resolution recognition in protein--protein complexes. Proc Natl Acad Sci U S A 1999; 96: 8477-82.

25. Mandell, JG, Roberts, VA, Pique, ME, Kotlovyi, V, Mitchell, JC, Nelson, E, Tsigelny, I, Ten Eyck, LF. Protein docking using continuum electrostatics and geometric fit. Protein Eng 2001; 14: 105-13.

26. Camacho, CJ, Gatchell, DW, Kimura, SR, Vajda, S. Scoring docked conformations generated by rigid-body protein-protein docking. Proteins 2000; 40: 525-37.

27. Nelsestuen, GL, Ostrowski, BG. Membrane association with multiple calcium ions: vitamin-K-dependent proteins, annexins and pentraxins. Curr Opin Struct Biol 1999; 9: 433-7.

28. Banner, DW, D'Arcy, A, Chène, C, Winkler, FK, Guha, A, Konigsberg, WH, Nemerson, Y, Kirchhofer, D. The crystal structure of the complex of blood coagulation factor VIIa with soluble tissue factor. Nature 1996; 380: 41-6.

29. Brandstetter, H, Bauer, M, Huber, R, Lollar, P, Bode, W. X-ray structure of clotting factor IXa: Active site and module structure related to Xase activity and hemophilia B. Proc. Natl. Acad. Sci. USA 1995; 92: 9796-800.

30. Zhong, D, Smith, KJ, Birktoft, JJ, Bajaj, SP. First epidermal growth factor-like domain of human blood coagulation factor IX is required for its activation by factor VIIa/tissue factor but not by factor XIa. Proc Natl Acad Sci U S A 1994; 91: 3574-8.

31. Chang, JY, Monroe, DM, Stafford, DW, Brinkhous, KM, Roberts, HR. Replacing the first epidermal growth factor-like domain of factor IX with that of factor VII enhances activity in vitro and in canine hemophilia B. J Clin Invest 1997; 100: 886-92.

32. Ruf, W, Shobe, J, Rao, SM, Dickinson, CD, Olson, A, Edgington, TS. Importance of factor VIIa Gla-domain residue Arg-36 for recognition of the macromolecular substrate factor X Gla-domain. Biochemistry 1999; 38: 1957-66.

33. Leonard, BJ, Clarke, BJ, Sridhara, S, Kelley, R, Ofosu, FA, Blajchman, MA. Activation and active site occupation alter conformation in the region of the first epidermal growth factor-like domain of human factor VII. J Biol Chem 2000; 275: 34894-900.

34. Jacobs, M, Freedman, SJ, Furie, BC, Furie, B. Membrane binding properties of the factor IX gamma-carboxyglutamic acid- rich domain prepared by chemical synthesis. J Biol Chem 1994; 269: 25494-501.

35. Sunnerhagen, M, Forsén, S, Hoffrén, A-M, Drakenberg, T, Teleman, O, Stenflo, J. Structure of the Ca^{2+}-free GLA domain sheds light on membrane binding of blood coagulation proteins. Nat. Struct. Biol. 1995; 2: 504-9.

36. Freedman, SJ, Blostein, MD, Baleja, JD, Jacobs, M, Furie, BC, Furie, B. Identification of the phospholipid binding site in the vitamin K-dependent blood coagulation protein factor IX. J. Biol. Chem. 1996; 271: 16227-36.

37. Ten Eyck, LF, Mandell, J, Roberts, VA, Pique, ME. in Proceedings of the 1995 ACM/IEEE Supercomputing Conference, San Diego, December 3-8, 1995 (Hayes, A., Simmons, M., eds) IEEE Computer Society Press, Los Alamitos, CA; http://www.supercomp.org/sc95/proceedings/636_LTEN/SC95.HTM.

38. Roberts, VA, Pique, ME. Definition of the interaction domain for cytochrome c on cytochrome c oxidase. III. Prediction of the docked complex by a complete, systematic search. J Biol Chem 1999; 274: 38051-60.

39. Brünger, AT. Book X-PLOR Manual. Version 3.0. (Editor, ed)^eds) New Haven: Yale University 1992;

40. Brooks, B, Bruccoleri, R, Olafson, B, States, D, Swaminathan, S, Karplus, M. CHARMM: A program for macromolecular energy, minimization, and molecular dynamics calculations. J. Comp. Chem. 1983; 4: 187-217.

41. O'Hara, PJ, Grant, FJ, Haldeman, BA, Gray, CL, Insley, MY, Hagen, FS, Murray, MJ. Nucleotide sequence of the gene coding for human factor VII, a vitamin K-dependent protein participating in blood coagulation. Proc. Natl. Acad. Sci. USA 1987; 84: 5158-62.

42. Yoshitake, S, Schach, BG, Foster, DC, Davie, EW, Kurachi, K. Nucleotide sequence of the gene for human factor IX (antihemophilic factor B). Biochemistry 1985; 24: 3736-50.

43. Leytus, SP, Foster, DC, Kurachi, K, Davie, EW. Gene for human factor X: A blood coagulation factor whose gene organization is essentially identical with that of factor IX and protein C. Biochemistry 1986; 25: 5098-102.

44. Pellequer, JL, Gale, AJ, Getzoff, ED, Griffin, JH. Three-dimensional model of the coagulation factor Va bound to activated protein C. Thromb. Haemost. 2000; 84: 849-57.

45. Zhang, E, St. Charles, R, Tulinsky, A. Structure of extracellular tissue factor complexed with factor VIIa inhibited with a BPTI mutant. J. Mol. Biol. 1999; 285: 2089-104.

46. Perera, L, Darden, TA, Pedersen, LG. Modeling human zymogen factor IX. Thromb Haemost 2001; 85: 596-603.

47. Kirchhofer, D, Lipari, MT, Moran, P, Eigenbrot, C, Kelley, RF. The tissue factor region that interacts with substrates factor IX and Factor X. Biochemistry 2000; 39: 7380-7.

48. Kumar, A, Blumenthal, DK, Fair, DS. Identification of molecular sites on factor VII which mediate its assembly and function in the extrinsic pathway activation complex. J Biol Chem 1991; 266: 915-21.

49. Mathur, A, Zhong, D, Sabharwal, AK, Smith, KJ, Bajaj, SP. Interaction of factor IXa with factor VIIIa. Effects of protease domain Ca2+ binding site, proteolysis in the autolysis loop, phospholipid, and factor X. J Biol Chem 1997; 272: 23418-26.

50. Chang, J, Jin, J, Lollar, P, Bode, W, Brandstetter, H, Hamaguchi, N, Straight, DL, Stafford, DW. Changing residue 338 in human factor IX from arginine to alanine causes an increase in catalytic activity. J Biol Chem 1998; 273: 12089-94.

51. Kolkman, JA, Mertens, K. Insertion loop 256-268 in coagulation factor IX restricts enzymatic activity in the absence but not in the presence of factor VIII. Biochemistry 2000; 39: 7398-405.

52. Celie, PH, Lenting, PJ, Mertens, K. Hydrophobic contact between the two epidermal growth factor-like domains of blood coagulation factor IX contributes to enzymatic activity. J Biol Chem 2000; 275: 229-34.

53. Shobe, J, Dickinson, CD, Ruf, W. Regulation of the catalytic function of coagulation factor VIIa by a conformational linkage of surface residue Glu 154 to the active site. Biochemistry 1999; 38: 2745-51.

54. Ruf, W. Factor VIIa residue Arg290 is required for efficient activation of the macromolecular substrate factor X. Biochemistry 1994; 33: 11631-6.

55. Wu, PC, Hamaguchi, N, Yu, YS, Shen, MC, Lin, SW. Hemophilia B with mutations at glycine-48 of factor IX exhibited delayed activation by the factor VIIa-tissue factor complex. Thromb Haemost 2000; 84: 626-34.

56. Hertzberg, MS, Facey, SL, Hogg, PJ. An Arg/Ser substitution in the second epidermal growth factor-like module of factor IX introduces an O-linked carbohydrate and markedly impairs

activation by factor XIa and factor VIIa/Tissue factor and catalytic efficiency of factor IXa. Blood 1999; 94: 156-63.

57. Huang, Q, Neuenschwander, PF, Rezaie, AR, Morrissey, JH. Substrate recognition by tissue factor-factor VIIa. Evidence for interaction of residues Lys165 and Lys166 of tissue factor with the 4- carboxyglutamate-rich domain of factor X. J Biol Chem 1996; 271: 21752-7.

58. Dittmar, S, Ruf, W, Edgington, TS. Influence of mutations in tissue factor on the fine specificity of macromolecular substrate activation. Biochem J 1997; 321: 787-93.

59. Ruf, W, Miles, DJ, Rehemtulla, A, Edgington, TS. Tissue factor residues 157-167 are required for efficient proteolytic activation of factor X and factor VII. J Biol Chem 1992; 267: 22206-10.

60. Ruf, W, Edgington, TS. An anti-tissue factor monoclonal antibody which inhibits TF.VIIa complex is a potent anticoagulant in plasma. Thromb Haemost 1991; 66: 529-33.

61. Kirchhofer, D, Eigenbrot, C, Lipari, MT, Moran, P, Peek, M, Kelley, RF. The tissue factor region that interacts with factor Xa in the activation of factor VII. Biochemistry 2001; 40: 675-82.

62. Kirchhofer, D, Moran, P, Chiang, N, Kim, J, Riederer, MA, Eigenbrot, C, Kelley, RF. Epitope location on tissue factor determines the anticoagulant potency of monoclonal anti-tissue factor antibodies. Thromb Haemost 2000; 84: 1072-81.

63. Huang, M, Syed, R, Stura, EA, Stone, MJ, Stefanko, RS, Ruf, W, Edgington, TS, Wilson, IA. The mechanism of an inhibitory antibody on TF-initiated blood coagulation revealed by the crystal structures of human tissue factor, Fab 5G9 and TF.G9 complex. J Mol Biol 1998; 275: 873-94.

64. Dickinson, CD, Shobe, J, Ruf, W. Influence of cofactor binding and active site occupancy on the conformation of the macromolecular substrate exosite of factor VIIa. J Mol Biol 1998; 277: 959-71.

65. Dennis, MS, Eigenbrot, C, Skelton, NJ, Ultsch, MH, Santell, L, Dwyer, MA, O'Connell, MP, Lazarus, RA. Peptide exosite inhibitors of factor VIIa as anticoagulants. Nature 2000; 404: 465-70.

66. Rusconi, CP, Yeh, A, Lyerly, HK, Lawson, JH, Sullenger, BA. Blocking the initiation of coagulation by RNA aptamers to factor VIIa. Thromb Haemost 2000; 84: 841-8.

67. Pawashe, AB, Golino, P, Ambrosio, G, Migliaccio, F, Ragni, M, Pascucci, I, Chiariello, M, Bach, R, Garen, A, Konigsberg, WK, et al. A monoclonal antibody against rabbit tissue factor inhibits thrombus formation in stenotic injured rabbit carotid arteries. Circ Res 1994; 74: 56-63.

68. Biemond, BJ, Levi, M, ten Cate, H, Soule, HR, Morris, LD, Foster, DL, Bogowitz, CA, van der Poll, T, Buller, HR, ten Cate, JW. Complete inhibition of endotoxin-induced coagulation activation in chimpanzees with a monoclonal Fab fragment against factor VII/VIIa. Thromb Haemost 1995; 73: 223-30.

69. Feuerstein, GZ, Patel, A, Toomey, JR, Bugelski, P, Nichols, AJ, Church, WR, Valocik, R, Koster, P, Baker, A, Blackburn, MN. Antithrombotic efficacy of a novel murine antihuman factor IX antibody in rats. Arterioscler Thromb Vasc Biol 1999; 19: 2554-62.

70. Kirchhofer, D, Tschopp, TB, Baumgartner, HR. Active site-blocked factors VIIa and IXa differentially inhibit fibrin formation in a human ex vivo thrombosis model. Arterioscler Thromb Vasc Biol 1995; 15: 1098-106.

71. Taylor, FB, Chang, AC, Peer, G, Li, A, Ezban, M, Hedner, U. Active site inhibited factor VIIa (DEGR VIIa) attenuates the coagulant and interleukin-6 and -8, but not tumor necrosis factor, responses of the baboon to LD100 Escherichia coli. Blood 1998; 91: 1609-15.

72. Ghrib, F, Leger, P, Ezban, M, Kristensen, A, Cambus, J, Boneu, B. Anti-thrombotic and haemorrhagic effects of active site-inhibited factor VIIa in rats. Br J Haematol 2001; 112: 506-12.

73. Himber, J, Kirchhofer, D, Riederer, M, Tschopp, TB, Steiner, B, Roux, SP. Dissociation of antithrombotic effect and bleeding time prolongation in rabbits by inhibiting tissue factor function. Thromb Haemost 1997; 78: 1142-9.

74. Bullens, S, Smith, N, Rowell, TJ, Chen, C, Hanson, S, Bunting, S. Safety and efficacy of a humanized anti-tissue factor antibody F(ab')2 fragment. Supplement to the journal Thrombosis and Haemostasis 2001; July 2001: abstract 1388.

75. Kraulis, PJ. MOLSCRIPT: a program to produce both detailed and schematic plots of protein structures. J. Appl. Cryst. 1991; 24: 946-50.

76. Merritt, EA, Bacon, DJ. Raster3D: Photorealistic molecular graphics. Meth. Enzymol. 1997; 277: 505-24.

Figure legends

Fig. 1: A, Ribbon representation of the docking orientation of FIX (orange and purple) onto FVIIa:TF complex (cyan and green). The orange conformation depicts the orientation identified by the docking program whereas the purple orientation is the computationally optimized docking. Calcium ions are drawn as grey spheres. The yellow line symbolizes the presence of a putative membrane plane. B, Stereo plot depicting specific side-chains involved in direct interactions between FVIIa:TF and FIX. Side-chains are displayed as ball and sticks following the colour scheme of the protein they belong to. The atom colour code is black for carbon, blue for nitrogen, and red for oxygen. Hydrogen bonds or salt bridges are shown as orange dotted lines. All figures were drawn using Molscript (75) and were rendered using Raster3D (76).

Fig. 2: Multiple sequence alignment of the N-terminal sequences of vitamin K-dependent coagulation factors. Highlighted residues are located at the interface between FVIIa:FIX or TF:FIX. Grey background residues (M/I/K18, D49, G60) are chemically conserved in FVII, FIX, FX, and APC. Residues highlighted in white (K22, Y45, N54, K63) are chemically conserved only in FVII, FIX, and FX. Dots represent a deletion that occurs in FVII, FIX, and FX compared with APC. Numbering corresponds to the mature FIX protein.

Fig. 3: CPK representation of the FVIIa:TF:FIX complex (cyan:green:purple). A, stereo view where hydrophobic solvent-exposed side-chains of FVIIa and FIX Gla domains are coloured in dark grey (bottom). FVIIa inhibitory peptide H142-H163(285-305) is coloured in red. B, back side view showing the complex 180° from A. FIX residues coloured in yellow are known to be in

contact with coagulation factors other than FVIIa, whereas the FIX catalytic triad is coloured in orange. C, Simplified view of the FVIIa:TF:FIX ternary complex.

Fig. 4: A) Stereo view of molecular steric hindrance between the FVIIa:TF:FIX ternary complex (cyan:green:purple) and the anti-coagulant anti-TF antibody 5G9 (transparent light grey CPK). Epitope residues of 5G9 have been coloured in red on TF (green). Antibody F3-3.2A binds FVIIa residues coloured in red. Epitope residues of FVIIa recognized by antibodies 12C7 and 12D10 have been coloured in yellow (top). B, Back side view of the complex 180° from A.

Fig. 5: Stereo plot showing the predicted structural mechanism of new anti-coagulant exosite peptides. The conformational change observed in the loop H142-H154 from the crystallographic structure of FVIIa-E76 peptide (code 1DVA) is drawn in orange, and is overlaid onto the FVIIa:TF crystal structure (code 1DAN). Activation peptide of FIX (purple) binds to FVIIa active site cleft (cyan) highlighted by the catalytic triad drawn in balls and sticks (top right). FIX cleavage site, residue Arg(180), is also drawn in purple balls and sticks. Steric clash between the activation peptide of FIX and FVIIa is indicated by the magenta arrow.

Figure 1

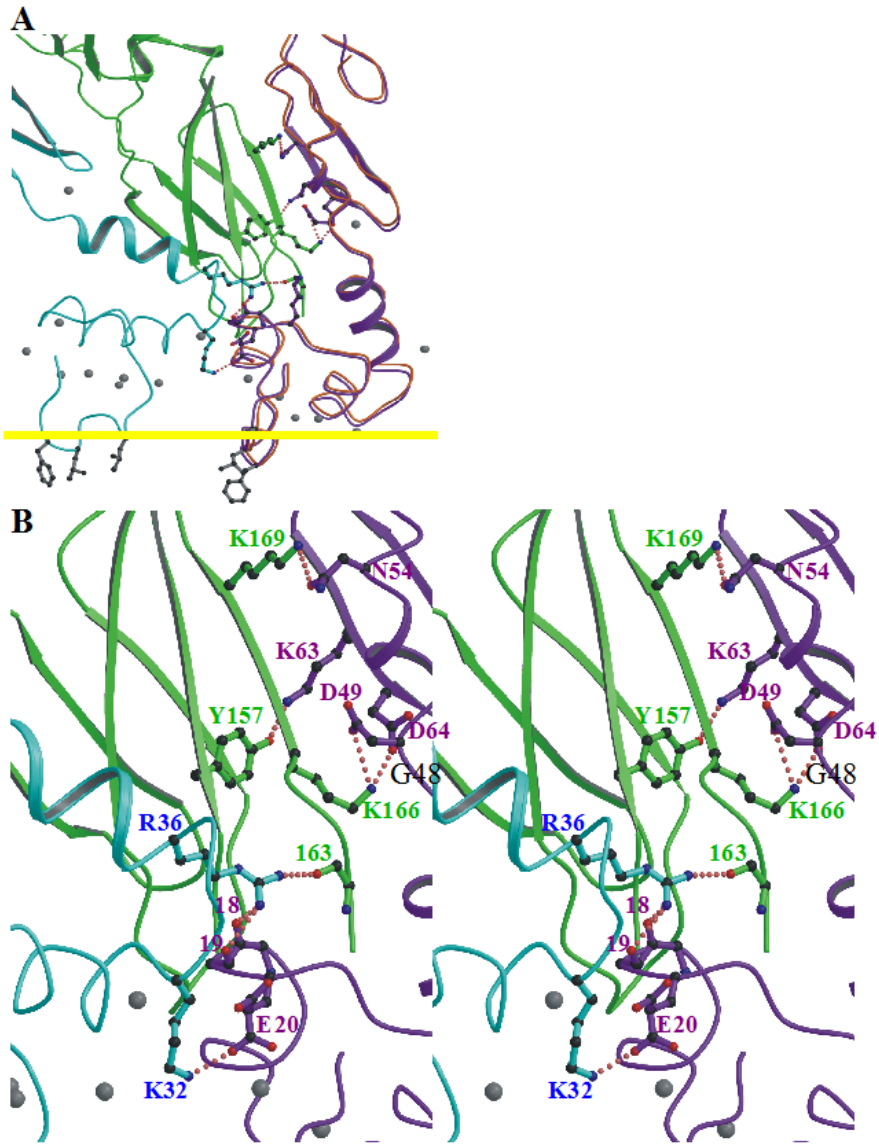
A
B
K169
N54
K63
D49
Y157
D64
G48
K166
R36
163
18
19
E20
K32
K169
N54
K63
D49
Y157
D64
G48
K166
R36
163
18
19
E20
K32

Figure 2

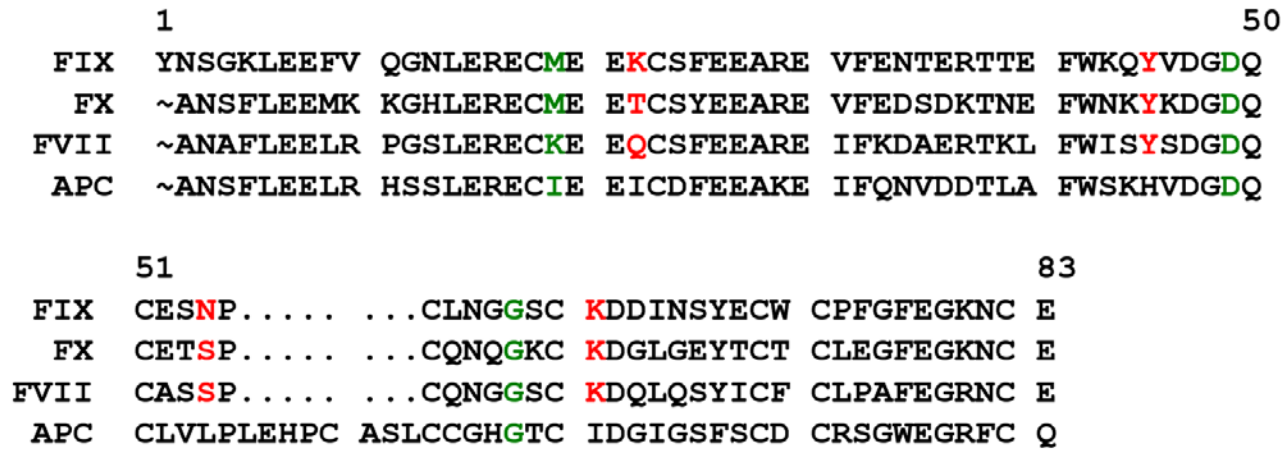
1 50
FIX YNSGKLEEFV QGNLERECME EKCSFEEARE VFENTERTTE FWKQYVDGDQ
FX ~ANSFLEEMK KGHLERECME ETCSYEEARE VFEDSDKTNE FWNKYKDGDQ
FVII ~ANAFLEELR PGSLERECKE EQCSFEEARE IFKDAERTKL FWISYSDGDQ
APC ~ANSFLEELR HSSLERECIE EICDFEEAKE IFQNVDDTLA FWSKHVDGDQ
51 83
FIX CESNP..... ...CLNGGSC KDDINSYECW CPFGFEGKNC E
FX CETSP..... ...CQNQGKC KDGLGEYTCT CLEGFEGKNC E
FVII CASSP..... ...CQNGGSC KDQLQSYICF CLPAFEGRNC E
APC CLVLPLEHPC ASLCCGHGTC IDGIGSFSCD CRSGWEGRFC Q

Figure 3

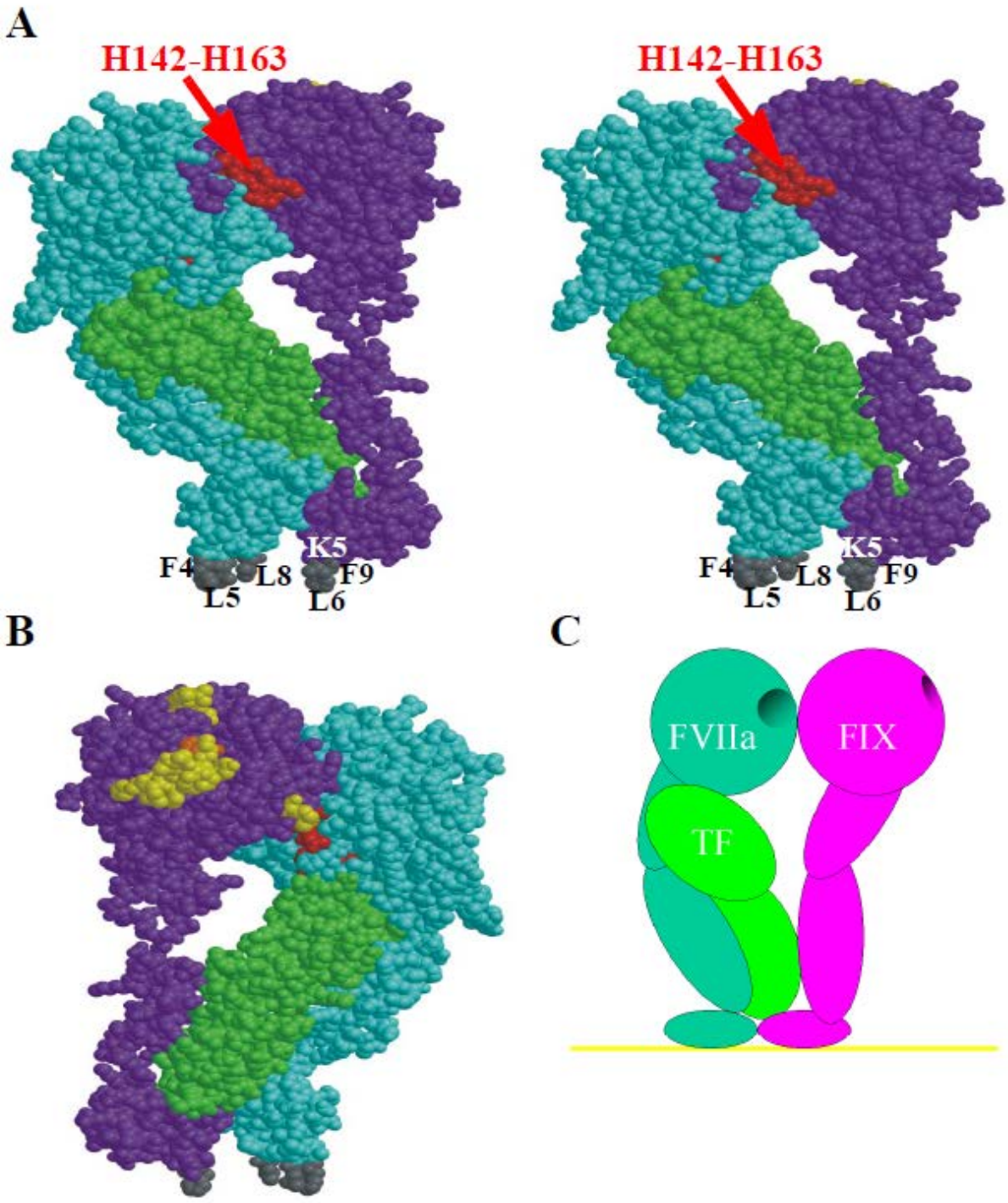
A
H142-H163
F4
L5
L8
K5
L6
F9
H142-H163
F4
L5
L8
K5
L6
F9
B
C
FVIIa
FIX
TF

Figure 4

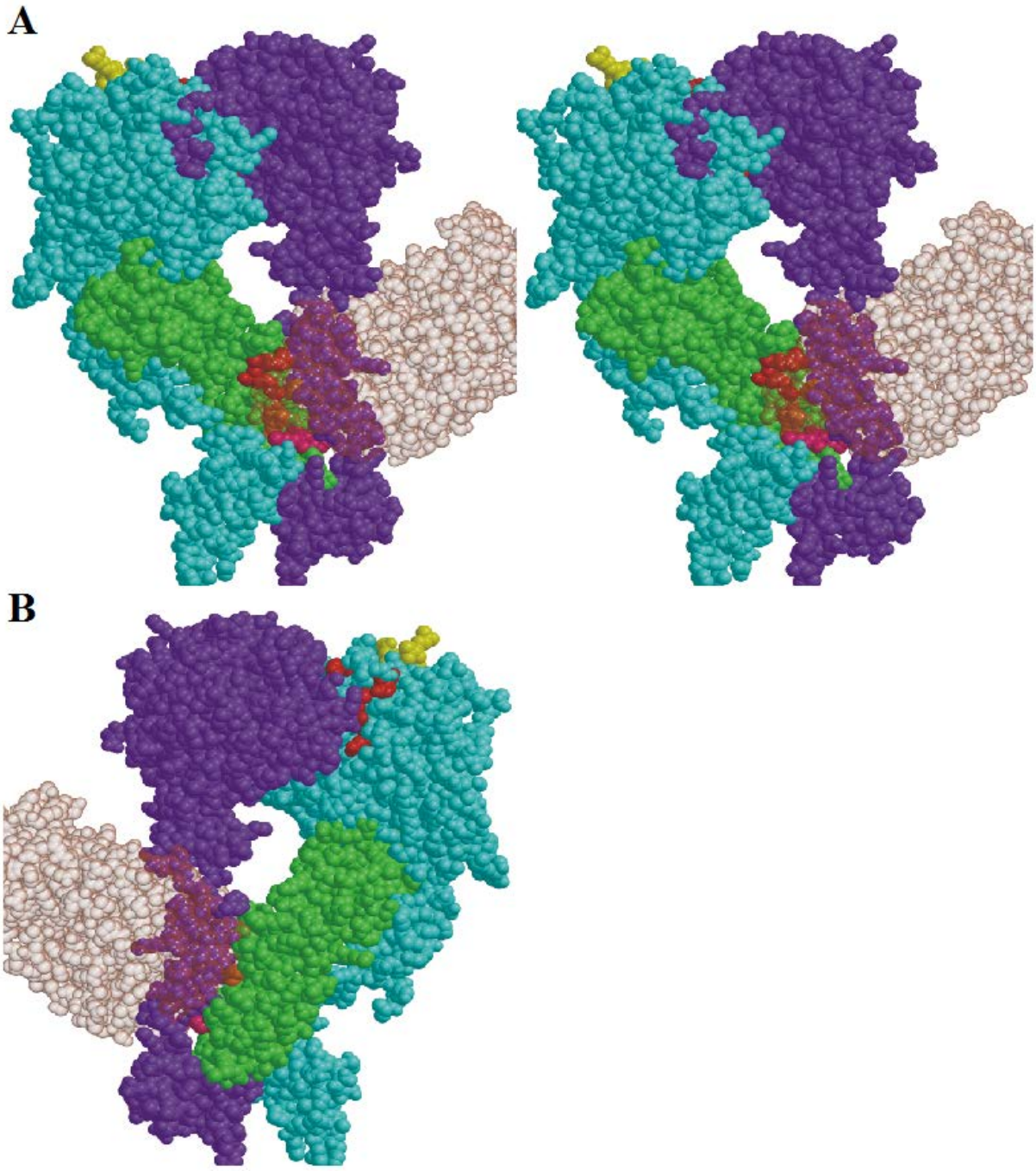

Figure 5